Journal of Luminescence 42 (1988) 275–282
North-Holland, Amsterdam

ON THE Gd^{3+} LUMINESCENCE AND ENERGY MIGRATION IN $Li(Y, Gd)F_4$–Tb^{3+}

A.J. De VRIES, M.F. HAZENKAMP and G. BLASSE

Physics Laboratory, University of Utrecht, P.O. Box 80000, 3508 TA Utrecht, the Netherlands

Received 31 May 1988
Revised 23 August 1988
Accepted 13 September 1988

The luminescence properties of the Gd^{3+} ion in $LiYF_4$ and the energy migration among the Gd^3 ions via the $^6P_{7/2}$ level and the $^6I_{7/2}$ level in the isostructural compound $LiGdF_4$ are reported. The isolated Gd^{3+} ions in this structure show efficient emission from the ^6I level. The non-radiative $^6I \rightarrow {}^6P$ relaxation can be ascribed by a 5-phonon relaxation process, involving 490 cm^{-1} phonons which are available from the A_u vibrational mode. The decay of the Gd^{3+} emission in $Li(Y, Gd)F_4$–Tb^{3+} can be described by a theory of energy migration developed by Burshtein et al. Parameters following from these fits indicate that the energy migration among the Gd^{3+} ions via the $^6P_{7/2}$ level and via the $^6I_{7/2}$ level is governed by exchange interaction. Parameters for the Gd^{3+}–Gd^{3+} and Gd^{3+}–Tb^{3+} transfer rates in this structure are given.

1. Introduction

During the last decades, the luminescence of rare earth ions in different host lattices has been studied extensively. In several compounds the rare earth ion luminescence is quenched due to energy migration among the rare earth ions followed by energy transfer to quenching centres or activator ions. The luminescence properties of some rare earth compounds have been applied successfully, e.g. as laser materials, as lamp phosphors or as X-ray phosphors [1–4]. In particular Gd^{3+} compounds are interesting from a fundamental and a practical point of view [5,6].

In an earlier study, the energy transfer phenomena in $Li(Y, Gd)F_4$–Ce, Tb were investigated in view of the probable application of this compound as a lamp phosphor. Parameters were estimated for the different transfer rates in this compound [7].

In this study we will focus on the luminescence of Gd^{3+} in $Li(Y, Gd)F_4$–Tb^{3+}. In sect. 3.1 the lower part of the energy level diagram of Gd^{3+} in $LiYF_4$–1%Gd^{3+} is determined. According to an earlier study, energy migration among the Gd^{3+} ions is absent at this low Gd^{3+} concentration [8]. Upon excitation in one of the components of the $^6I_{7/2}$ level, emission from the ^6I level of Gd^{3+} is observed. The occurrence of this emission is explained by a slow $^6I \rightarrow {}^6P$ non-radiative relaxation process involving 5 phonons. In sect. 3.2 the time dependence of the Gd^{3+} $^6P_{7/2}$ and $^6I_{7/2}$ emission in $LiY_{1-x}Gd_xF_4$–Tb^{3+} ($0.1 < x < 1$) is evaluated in terms of the microparameters for donor–donor (C_{dd}) and donor–acceptor (C_{da}) interaction, using the theory of energy migration developed by Burshtein et al. The donor–donor and donor–acceptor transfers are dominated by exchange interaction.

$LiYF_4$ and $LiGdF_4$ are isostructural and have the (inverse) scheelite structure. The site symmetry of the Y^{3+} and Gd^{3+} site is S_4 [9].

2. Experimental

Powder samples of $LiY_{0.99}Gd_{0.01}F_4$, $LiY_{0.99-x}Gd_xTb_{0.01}F_4$ ($x = 0.10$, 0.20, 0.30, 0.40, 0.50, 0.60, 0.70, 0.80, 0.90, 0.99), $LiGd_{1-y}Tb_yF_4$ ($y = 0$, 0.003, 0.006, 0.01), $LiY_{0.999-x}Gd_xTb_{0.001}F_4$ ($x = 0.200$, 0.400, 0.500, 0.600, 0.700, 0.900, 0.999), and $LiY_{0.99-x}Gd_xTm_{0.01}F_4$ ($x = 0.10$, 0.20, 0.30, 0.40, 0.50, 0.60, 0.70, 0.80, 0.90, 0.99) were prepared by a method described in ref. [7]. The

samples were checked by X-ray powder diffraction using CuKα radiation.

The optical and decay measurements were performed on a Nd–YAG laser set-up described in detail in ref. [10]. The frequency-doubled output of the laser excited a tunable dye laser. The output of the dye laser was doubled again to obtain UV emission. The linewidth at 280 nm was smaller than 0.5 cm^{-1}. The sample was mounted in an Oxford MD4 Bath Cryostat equipped with an ITC4 temperature controller. The temperature of the sample could be varied in the range 1.2–300 K.

3. Results and discussion

3.1. $LiYF_4$–1%Gd^{3+}

From the excitation spectrum of the lowest energy Gd^{3+} emission line at 32113 cm^{-1}, the positions of the $^6P_{7/2}$, $^6P_{5/2}$, $^6P_{3/2}$ and $^6I_{7/2}$ energy levels of Gd^{3+} could be determined. In table 1 their positions are given. In $LiYF_4$–1%Gd the Gd^{3+} ion occupies the Y^{3+} site. The number of crystal-field components of the $^6P_{7/2}$, $^6P_{5/2}$, $^6P_{3/2}$ and $^6I_{7/2}$ levels amounts to 4, 3, 2 and 4, respectively. This agrees with the site symmetry of the Y^{3+} site.

At 298 K, excitation in one of the crystal-field components of the $^6P_{7/2}$ or $^6P_{5/2}$ level yields a strong emission from the $^6P_{7/2}$ level and a weak emission from the $^6P_{5/2}$ level. At this temperature the $^6P_{5/2}$ level is thermally populated. At 4.2 K excitation in the same levels yields emission from the lowest energy crystal-field component of the $^6P_{7/2}$ level only. The emission spectrum after excitation in one of the crystal field components of the $^6I_{7/2}$ level at 298 K, is given in fig. 1. Emission from the $^6P_{7/2}$ and $^6P_{5/2}$ levels of Gd^{3+} and emission from the crystal-field components of the ^6I_J levels of Gd^{3+} are observed. At this temperature the ^6I_J levels are thermally populated. Upon excitation in the $^6I_{7/2}$ level at 4.2 K, only emission from the lowest energy $^6I_{7/2}$ component and emission from the lowest energy $^6P_{7/2}$ component are observed.

Table 1
Location of the crystal field components of the $^6P_{7/2}$, $^6P_{5/2}$, $^6P_{3/2}$ and $^6I_{7/2}$ levels of Gd^{3+} in $LiYF_4$–1%Gd^{3+} (values in cm^{-1})

Level	Location	Level	Location
$^6P_{7/2}$	32112.7	$^6P_{3/2}$	33309
	32153.2		33338
	32172.0		
	32173.7	$^6I_{7/2}$	35844
			35865
$^6P_{5/2}$	32709.1		35892
	32756.0		35945
	32768.1		

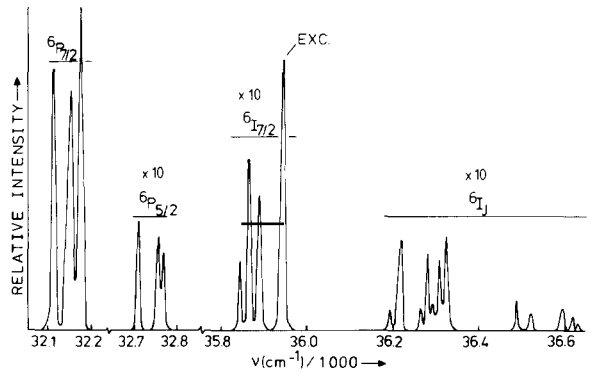

Fig. 1. Emission spectrum at 298 K of Gd^{3+} in $LiYF_4$–1%Gd^{3+} upon excitation in the component of the $^6I_{7/2}$ level at 35945 cm^{-1}. Note breaks in the wavelength scale. The laser excitation is indicated. The intensity of the corresponding emission contains a contribution of the exciting laser pulse.

In compounds where energy migration among the Gd^{3+} ions is absent, emission from the Gd^{3+} $^6I_{7/2}$ level can be expected if the non-radiative $^6I \rightarrow {}^6P$ relaxation rate (K_{nr}) is low compared to the radiative decay rate of the $^6I_{7/2}$ level ($K_r(^6I)$. The ratio $K_r(^6I)/K_{nr}$ is equal to the ratio Int(^6I)/Int(^6P), where Int(^6I) (Int(^6P)) is the total amount of Gd^{3+} $^6I(^6P)$ emission upon excitation in one of the components of the ^6I manifold of Gd^{3+}. The decay time of the $^6I_{7/2}$ level upon excitation in one of the components of the ^6I manifold (τ) is equal to

$$1/\tau = K_{nr} + K_r(^6I). \quad (1)$$

Non-radiative transitions to the ground level $^8S_{7/2}$ are neglected in view of the large energy gap involved. The ratio Int(^6I)/Int(^6P) and τ were

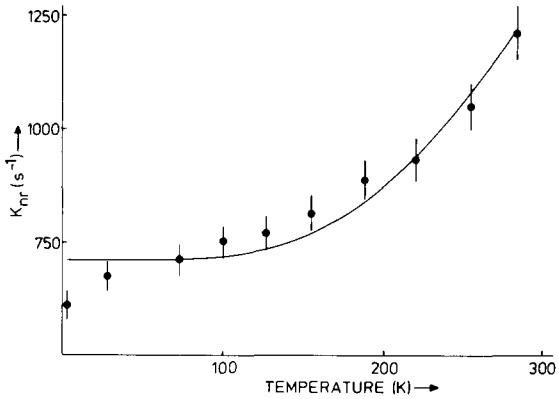

Fig. 2. The non-radiative Gd^{3+} $^6I \rightarrow {}^6P$ relaxation rate K_{nr} in $LiYF_4$–1%Gd^{3+} as a function of temperature. The drawn line is a fit to eq. (2).

measured as functions of the temperature T. The resulting values of K_{nr} are plotted in fig. 2. $K_r(^6I)$ at 4.2 K = 48.6 s^{-1}. The temperature dependence of the non-radiative multi-phonon relaxation rate K_{nr} is given by [11]

$$K_{nr}(T) = K_{nr}(0)(n+1)^p, \quad (2)$$

where $K_{nr}(T)$ is the non-radiative relaxation rate at temperature T, p is the number of phonons involved in the relaxation and n is given by

$$n = (\exp(E/pkT) - 1)^{-1}, \quad (3)$$

where E is the energy difference between the levels involved in the relaxation. The most reliable fit for K_{nr} as a function of the temperature was obtained for $p = 5$ and $E = 2370$ cm^{-1} (the drawn line in fig. 2). The energy difference involved in the $^6I \rightarrow {}^6P$ non-radiative relaxation is the energy difference between the lowest component of the $^6I_{7/2}$ level and the highest component of the $^6P_{3/2}$ level. From table 1 it can be seen that this energy difference is 2506 cm^{-1}. This value is in good agreement with the fit value for E. The energy of the phonons involved in the transition $E/p = 501$ cm^{-1}. This energy corresponds to the highest-energy lattice vibrations of $LiYF_4$, viz. 490 ± 10 cm^{-1} for the infrared active A_u mode. This mode belongs to a vibration of the Li^+ ions relative to the other ions [12]. An estimation of the multiphonon $^6I \rightarrow {}^6P$ relaxation rate using the modified energy gap law yields $K_{nr} = 7 \times 10^{3\pm1}$ s^{-1} [13]. The agreement with the experimental values is good.

Upon excitation in one of the components of the $^6P_{5/2}$ level at 4.2 K, the decay of the $^6P_{7/2}$ emission is found to be exponential; this yields a decay time of 9.6 ± 0.1 ms. To compare this value and the value of K_r with similar values in other host lattices, table 2 gives values for the radiative decay rates of the $^6I_{7/2}$ and the $^6P_{7/2}$ levels of Gd^{3+} in different host lattices. In this table, $LaAlO_3$–2%Gd is taken as an example for Gd^{3+} in an oxidic compound. In other oxidic compounds with a non-centrosymmetric site for the Gd^{3+} ion, similar decay rates for the $^6P_{7/2}$ level have been reported [15,16]. In $Cs_2NaGdCl_6$ the transitions within the $4f^7$ configuration of Gd^{3+} have a magnetic-dipole origin. Electric dipole transitions are forbidden due to the centrosymmetric site of the Gd^{3+} ion in this compound. For Gd^{3+} in the fluoride, the electric-dipole contribution to both decay rates is smaller than for Gd^{3+} in an oxidic compound on a non-centrosymmetric site. The position of the Gd^{3+} 5d level is the reason for this difference. In general, in fluorides the 5d level of Gd^{3+} lies at a higher energy than in oxides [17]. The admixture of 5d wavefunctions into the 4f wavefunctions by odd terms in the crystal-field expansion is responsible for the forced electric-dipole transitions within the $4f^7$ configuration. Therefore, in oxides the electric-dipole contribution is larger than in fluorides. The same argument has been used to explain the different ranges of energy transfer between Gd^{3+} ions in fluorides and oxides [8]. The radiative decay rate of the $^6I_{7/2}$ level is more sensitive to this change than the rate of the $^6P_{7/2}$ level, since the $^6I_{7/2} \rightarrow$

Table 2
Radiative decay rates of the $^6P_{7/2}$ and $^6I_{7/2}$ levels of Gd^{3+} in different host lattices (values in s^{-1})

	$^6P_{7/2}$	$^6I_{7/2}$	T
$Cs_2NaGdCl_6$ [a]	77	<1	4.2 K
$LiYF_4$–1%Gd^{3+} [b]	104	48.6	4.2 K
	115	142	300 K
$LaAlO_3$–2%Gd^{3+} [c]	345	570	300 K

[a] Ref. [14];
[b] This work;
[c] Ref. [10].

$^8S_{7/2}$ transition is only allowed as a magnetic-dipole transition by the deviation from LS coupling [14].

3.2. Li(Y, Gd)F_4–Tb^{3+}

In this section parameters for the Gd^{3+}–Gd^{3+} and Gd^{3+}–Tb^{3+} energy transfer are derived from the decay of the Gd^{3+} $^6P_{7/2}$ and $^6I_{7/2}$ emission. First a model is presented which is used to describe the Gd^{3+} decay curves and to derive these parameters.

3.2.1. Model

It has been shown before that the theory of excited state relaxation processes, which was developed by Burshtein et al. can be applied successfully to the evaluation of the energy transfer parameters in Gd^{3+} compounds [18]. This theory predicts that the decay of the donor emission (i.e. the Gd^{3+} emission) can be described by one formula which is valid for different regimes. The donor emission becomes exponential for longer times after the excitation pulse. This exponential part can be represented by

$$I(t) = I(0)\exp[-t/\tau_0 - Wt - \Delta], \tag{4}$$

where $1/\tau_0$ is the decay rate of the isolated donor ion, W a parameter which characterizes the donor–acceptor (i.e. the Gd^{3+}–Tb^{3+}) energy transfer preceded by energy migration among the donor ions and $\exp(-\Delta)$ represents the portion of the excitation energy which is not lost by direct transfer. For W the following expression is valid for all migration mechanisms, viz. [19]:

$$W = y\sum_{i=1}^{\infty} W_{da} n(R_i), \tag{5}$$

where y is the relative acceptor concentration, the summation is over the lattice sites in the donor–acceptor sublattice, W_{da} is the donor–acceptor transfer rate ($W_{da} = C_{da} f(R)$ [19]) and $n(R_i)$ is the steady-state excitation density which is equal to [19]

$$n(R_i) = (1 + W_{da}\tau_1)^{-1}. \tag{6}$$

$1/\tau_1$ is the maximum probability for energy transfer between two donor ions. For donor–donor transfer via dipole–dipole interaction $1/\tau_1$ can be expressed by [20]

$$1/\tau_1 = 8\pi^3 N_D^2 C_{dd}/27, \tag{7}$$

where N_D is the donor–ion density and C_{dd} is the donor–donor interaction parameter. For donor–donor transfer via exchange interaction $1/\tau_1$ can be expressed by [20]

$$1/\tau_1 = 2C_{dd}\exp\left[-1.563 N_D^{-1/3} L_{dd}^{-1}\right], \tag{8}$$

where L_{dd} is the effective Bohr radius for donor–donor interaction.

Using this expression for $1/\tau_1$, four expressions for W can be derived for different interaction mechanisms between donor ions mutually and donor and acceptor ions.

– For donor–donor and donor–acceptor transfer via dipole–dipole interaction:

$$W = yC_{da}\sum_{i=1}^{\infty} R_i^{-6}/\left[1 + 0.109 C_{da}/\left(C_{dd} N_D^2 R_i^6\right)\right]; \tag{9}$$

– for donor–donor transfer via dipole–dipole interaction and donor–acceptor transfer via exchange interaction:

$$W = yC_{da}\sum_{i=1}^{\infty} \exp(-2R_i/L_{da}) \Big/\left[1 + 0.109 C_{da}\exp(-2R_i/L_{da})/\left(C_{dd} N_D^2\right)\right], \tag{10}$$

where L_{da} is the effective Bohr radius for donor–acceptor interaction;

– for donor–donor and donor–acceptor transfer via exchange interaction:

$$W = yC_{da}\sum_{i=1}^{\infty} \exp(-2R_i/L_{da}) \Big/\left[1 + C_{da}\exp(-2R_i/L_{da}) \Big/\left(2C_{dd}\exp\left\{-1.563 N_D^{-1/3} L_{dd}^{-1}\right\}\right)\right]; \tag{11}$$

– for donor–donor transfer via exchange interaction and donor–acceptor transfer via dipole–dipole interaction:

$$W = yC_{da}\sum_{i=1}^{\infty} R_i^{-6}/\left[1 + C_{da} \Big/\left(2C_{dd}\exp\left\{-1.563 N_D^{-1/3} L_{dd}^{-1}\right\} R_i^6\right)\right]. \tag{12}$$

3.2.2. Energy migration via the $^6P_{7/2}$ level

The decay of the Gd^{3+} $^6P_{7/2}$ level in $LiY_{0.99-x}Gd_xF_4$–1%Tb ($x = 0.1$, 0.2, 0.3, 0.4, 0.5, 0.6, 0.7, 0.8, 0.9, 0.99) at 298 K was measured upon excitation in one of the components of the $^6P_{5/2}$ level. For longer times after the excitation pulse all decay curves became exponential. In fig. 3 decay curves for different Gd^{3+} concentrations are plotted. The exponential part was fitted to eq. (4) with $\tau_0 = 8.7$ ms (the radiative decay time at 298 K). The resulting values of W vs N_D are given in fig. 4. These data were fitted to all equations for W derived in the previous section. The best fit was obtained for eq. (11) (donor–donor and donor–acceptor transfer via exchange interaction). In fig. 5 also the best fits for eqs. (9) (10) and (12) are given. The parameters following from the best fit are: $L_{dd} = L_{da} = 0.40$ Å, $C_{dd} = 12.2 \times 10^{13}$ s^{-1} and $C_{da} = 3.37 \times 10^{13}$ s^{-1}. The result that the Gd^{3+}–Gd^{3+} transfer in $LiGdF_4$ is governed by exchange is in line with conclusions in other studies on the energy migration in $LiGdF_4$, although these conclusions were based on more qualitative arguments [7,8]. The value of the Bohr radius is in agreement with literature data [21].

It is possible to calculate C_{da} in a different way. This method has been used before to diminish the influence of other activator and/or quenching ions on the value of C_{da} [18]. It is based on the linear

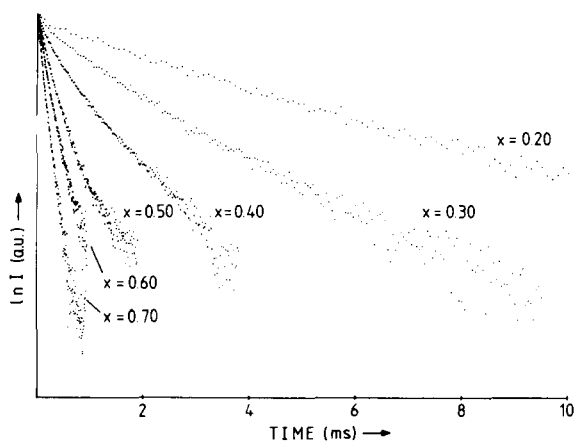

Fig. 3. Decay curves of the Gd^{3+} $^6P_{7/2}$ emission in $Li(Y_{0.99-x}, Gd_x)F_4$–1%Tb^{3+} at 300 K. Excitation is in the component of the $^6P_{5/2}$ level at 32768.1 cm^{-1}.

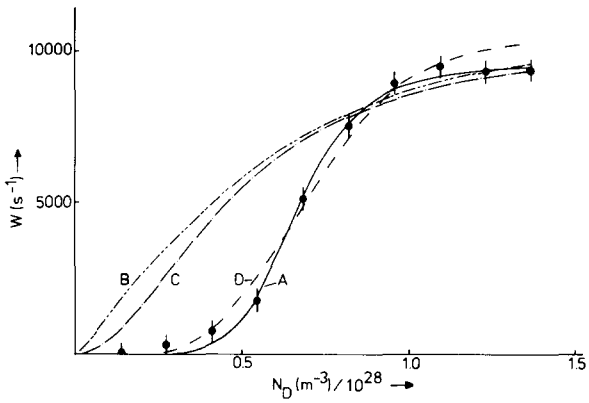

Fig. 4. Concentration dependence of the fit parameter W of the Gd^{3+} $^6P_{7/2}$ emission decay curves in Li(Y, Gd)F_4–1%Tb^{3+}. (A) fit to eq. (11); (B) fit to eq. (9); (C) fit to eq. (10); (D) fit to eq. (12).

dependence of W on y. For high donor concentrations and for $C_{da}/C_{dd} < 1$ the following is valid:

$$W = yC_{da}\sum_{i=1}^{\infty} R_i^{-6} \tag{13}$$

for donor–acceptor transfer via dipole–dipole interaction, and

$$W = yC_{da}\sum_{i=1}^{\infty} \exp(-2R_i/L_{da}) \tag{14}$$

for donor–acceptor transfer via exchange interaction. However, this method does not give any information about the interaction mechanism between donor and acceptor ions.

The decay of the Gd^{3+} emission in $LiGd_{1-y}Tb_yF_4$ ($y = 0$, 0.003, 0.006, 0.01) upon

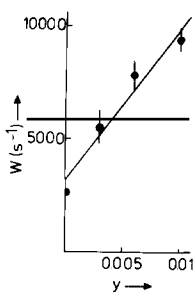

Fig. 5. Concentration dependence of the fit parameter W of the Gd^{3+} $^6P_{7/2}$ emission decay curves in $Li(Gd_{1-y}Tb_y)F_4$ at 298 K. The drawn line gives the linear dependence of W upon y.

excitation in the $^6P_{5/2}$ level was measured and fitted. The values of W resulting from these fits are given in fig. 5. The linear dependence of W gives $W = (6.72 \times 10^5 \quad y + 3106)\ s^{-1}$. For donor–acceptor transfer via exchange interaction and $L_{da} = 0.40$ Å, it follows that $C_{da} = 2.38 \times 10^{13}$ s^{-1}. This value of C_{da} is only a little smaller than the value of C_{da} derived from the dependence of W upon N_D. This indicates that the influence of other activator and/or quenching ions on the energy migration among the Gd^{3+} ions is small. In the following $C_{da} = 2.38 \times 10^{13}$ s^{-1} will be used as the parameter for donor–acceptor transfer.

With these quantitative results it is possible to calculate the nearest and next-nearest neighbour donor–donor transfer rates ($W_{nn(dd)}$ and $W_{nnn(dd)}$, respectively) and to check earlier conclusions on the energy migration in $LiGdF_4$, viz. that the energy migration concerns nearest neighbours only. In $LiGdF_4$ each Gd^{3+} ion has 4 nearest neighbours at 3.75 Å and 4 next-nearest neighbours at 5.19 Å [9]. Using $W_{dd} = C_{dd} \exp(-2R/L_{dd})$, it follows $W_{nn(dd)} = 8.78 \times 10^5$ s^{-1} and $W_{nn(dd)} = 655$ s^{-1}. The radiative decay rate of the $^6P_{7/2}$ level ($K_r(^6P)$) is 115 s^{-1}. Since $W_{nn(dd)} \gg W_{nnn(dd)}$, $K_r(^6P)$, energy migration in $LiGdF_4$ is dominated by energy migration via nearest Gd^{3+} neighbours. This holds also for the diluted system Li(Y, Gd)F_4, since $W_{nnn(dd)}$ is only slightly larger than $K_r(^6P)$. This result agrees well with an earlier conclusion derived from the critical Gd^{3+} concentration for migration [8].

The nearest-neighbour donor–acceptor transfer rate can be calculated in the same way as $W_{nn(dd)}$ and results in a value $W_{nn(da)} = 1.71 \times 10^5$ s^{-1}. The present values of $W_{nn(dd)}$ and $W_{nn(da)}$ are in fair agreement with those derived earlier in a completely different way [7]. The average number of steps in the migration process among the Gd^{3+} ions in $LiGdF_4$–1%Tb is $4 \times 0.99 W_{nn}/(4 \times 0.01 W_{nn(da)} + 1/\tau_0(^6P)) = 500$ steps. The mean diffusion length is equal to $\sqrt{(500)} \times R_{nn} = 83.9$ Å. In pure $LiGdF_4$ (i.e. without any activator and/or killer ion) this would be 30 540 steps and 656 Å, respectively.

Transfer via exchange interaction is governed by two factors, viz. a wavefunction overlap and a spectral overlap. The wavefunction overlap for both interactions is nearly equal, since Gd^{3+} and Tb^{3+} are both rare earth ions and neighbours in the periodic table. For Gd^{3+}–Gd^{3+} transfer the spectral overlap is much larger than for Gd^{3+}–Tb^{3+} transfer since the Gd^{3+}–Gd^{3+} transfer is resonant, or nearly resonant, whereas the Gd^{3+}–Tb^{3+} transfer is not. Therefore, one would expect a much larger transfer rate for Gd^{3+}–Gd^{3+} transfer than for Gd^{3+}–Tb^{3+} transfer. Obviously this is not the case. However, exchange interaction involves the mixing-in of a state with considerably higher energy which has both electrons involved at one of the two ions. It is possible to estimate the energy difference between the X^{4+}–Gd^{2+} state (X = Gd or Tb) and the X^{3+}–Gd^{3+} state by using the values of the standard reduction potentials as given by Carnall [22], viz. −11.8 and −7.2 V for Gd^{4+}–Gd^{2+} and Tb^{4+}–Gd^{2+}, respectively. This means that the state which has to be mixed in is at lower energy for the Gd^{3+}–Tb^{3+} couple. The larger spectral overlap for the Gd^{3+}–Gd^{3+} couple is therefore counteracted by the less effective mixing-in of the transferred state.

Upon excitation in the $^6P_{5/2}$ level of Gd^{3+} at 4.2 K not only emission from intrinsic Gd^{3+} ions is observed, but also from extrinsic Gd^{3+} ions, the so-called Gd^{3+} traps. This has been observed in several other compounds [10,15,16] and confirms the energy migration among the Gd^{3+} ions. At least 4 different traps were found with a maximum trap depth of 130 cm^{-1}.

3.2.3. *Energy migration via the $^6I_{7/2}$ level*

The decay of the lowest energy component of the Gd^{3+} $^6I_{7/2}$ level in $LiY_{0.999-x}Gd_xF_4$–0.1%Tb^{3+} ($x = 0.200$, 0.400, 0.500, 0.600, 0.700, 0.800 and 0.999) and $LiY_{0.99-x}F_4$–1%Tm^{3+} ($x = 0.10$, 0.20, 0.30, 0.40, 0.50, 0.60, 0.70, 0.80, 0.90 and 0.99) at 298 K was measured upon excitation in one of the higher energy components of the same level. For $x > 0.5$ the decay of the $^6I_{7/2}$ level consisted of a fast and a slower part. The decay time of the slower part does not depend on the Gd^{3+} concentration in a consequent way. It does not depend on the temperature nor on the laser power, so that its origin is not clear. Its influence on the fast component is negligible since the slow component has a much weaker intensity.

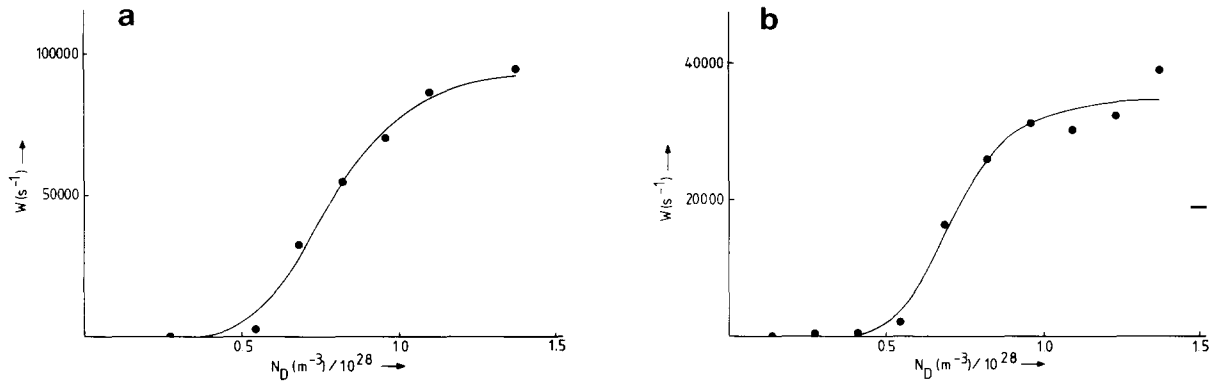

Fig. 6. Concentration dependence of the fit parameter W of the Gd^{3+} $^6I_{7/2}$ emission decay curves at 298 K in (a) Li(Y, Gd)F_4–0.1%Tb^{3+} and (b) Li(Y, Gd)F_4–1%Tm^{3+}. The drawn line gives a fit to eq. (11).

The decay of the fast part depends strongly on the Gd^{3+} concentration and is nearly one-exponential. This decay was fitted to eq. (4) with $\tau_0 = 0.82$ ms (the decay time of the $^6I_{7/2}$ level at 298 K in $LiYF_4$–1%Gd^{3+}). The resulting values of W vs. N_D are given in fig. 6. The values of W vs. N_D were fitted to eqs. (9–12). The best fit was obtained for donor–donor and donor–acceptor transfer via exchange interaction. The parameters following from this fit are given in table 3. The energy migration via the $^6I_{7/2}$ level in $LiGdF_4$ is governed by exchange interaction also. The fit value for the Bohr radius is again close to the literature value [21]. In the same way as in sect. 3.2.2. the values of $W_{nn(dd)}$ and $W_{nn(da)}$ were calculated. These values are also given in table 3.

The difference in the values for $W_{nn(dd)}$ for the Tb^{3+} and Tm^{3+} samples is remarkable, because this parameter describes a process which is the same in both samples. This difference can be explained in the following qualitative way.

Table 3
Parameters for the energy transfer and energy migration via the Gd^{3+} $^6P_{7/2}$ and $^6I_{7/2}$ level in $LiGdF_4$–Tb^{3+}/Tm^{3+}

	Tb^{3+} ($^6P_{7/2}$)	Tb^{3+} ($^6I_{7/2}$)	Tm^{3+}
L_{dd} (Å)	0.40	0.42	0.36
L_{da} (Å)	0.40	0.42	0.36
C_{dd} (S^{-1})	1.22×10^{14}	1.62×10^{15}	2.78×10^{15}
C_{da} (S^{-1})	2.38×10^{13}	1.38×10^{15}	9.90×10^{14}
$W_{nn(dd)}$ (S^{-1})	8.78×10^{5}	2.80×10^{7}	2.44×10^{6}
$W_{nn(da)}$ (S^{-1})	1.71×10^{5}	2.39×10^{7}	8.68×10^{5}

Both Tb^{3+} and Tm^{3+} have energy levels nearly resonant with the $^6I_{7/2}$ level of Gd^{3+} [23]. For Tb^{3+}, between this level and the lower energy emitting $^5D_3$ level, many other energy levels are situated. Fast non-radiative relaxation by a multi-phonon process from the higher energy levels to the $^5D_3$ level seems probable. For Tm^{3+} however, the situation is different. The $^3P_0$ level is nearly resonant with the $^6I_{7/2}$ level of Gd^{3+}. The next lower energy level of Tm^{3+} is the $^1D_2$ level at approximately 7000 cm^{-1} lower energy [23]. Non-radiative relaxation from the $^3P_0$ level to the $^1D_2$ level by multi-phonon emission seems improbable in view of the results in sect. 3.1. Back transfer from the $^3P_0$ level of Tm^{3+} to the $^6I_{7/2}$ level of Gd^{3+} is possible now. Therefore, the transfer rates in $LiGdF_4$–Tm^{3+} are effective rates influenced by the back transfer from Tm^{3+} to Gd^{3+}.

The Gd^{3+}–Gd^{3+} transfer rate via the $^6I_{7/2}$ is larger than the same transfer rate via the $^6P_{7/2}$ level. The difference is probably caused by the larger spectral overlap for energy migration via the $^6I_{7/2}$ level.

The average number of steps in the migration process among the Gd^{3+} ions via the $^6I_{7/2}$ level in $LiGdF_4$–0.1%Tb^{3+} is $4 \times 0.999W_{nn(dd)}/[4 \times 0.001W_{nn(da)} + 1/\tau_0(^6I)] = 1150$ steps; the mean diffusion length is $\sqrt{(1150)} \times R_{nn} = 127$ Å. In pure

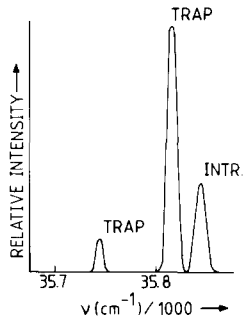

Fig. 7. $^6I_{7/2}$ emission spectrum of Gd^{3+} in $LiGdF_4$–1%Tb^{3+} at 4.2 K. Excitation is in the highest energy component of the $^6I_{7/2}$ level at 35945 cm^{-1}.

$LiGdF_4$ this would be 91900 steps and 1150 Å, respectively.

Energy migration among the Gd^{3+} ions via the $^6I_{7/2}$ level is possible due to the slow $^6I \rightarrow {}^6P$ non-radiative relaxation. The Gd^{3+}–Gd^{3+} $^6I_{7/2}$ transfer rate competes favourably with this relaxation, which makes energy migration via the $^6I_{7/2}$ level possible.

Another confirmation of the energy migration via the $^6I_{7/2}$ level of Gd^{3+} is found at lower temperatures. Figure 7 gives the Gd^{3+} $^6I_{7/2}$ emission in $LiGdF_4$–Tb^{3+} at 4.2 K. Upon excitation in the $^6I_{7/2}$ level at 4.2 K, not only the $^6I_{7/2}$ emission reported in sect. 3.1. was found, but also some extra emission peaks at a lower energy than the emission from intrinsic Gd^{3+} ions. This extra emission arises from Gd^{3+} traps (see above for trap emission after excitation in the $^6P_{7/2}$ level). At least 2 different ^6I traps were found with a maximum trap depth of 98 cm^{-1}.

Acknowledgements

The investigations were supported in part by the Netherlands Foundation for Chemical Research (SON) with financial aid from the Netherlands Technology Foundation (STW).

References

[1] G. Boulon, Rev. Phys. Appl. 21 (1986) 689.
[2] G. Blasse, ed., Mat. Chem. Phys. 16 (1987) 3–371.
[3] M.J.J. Lammers, Thesis, University Utrecht (1986).
[4] G. Blasse, Recl. Trav. Chim. Pays-Bas 105 (1986) 143.
[5] See e.g. G. Blasse, H.S. Kiliaan and A.J. de Vries, J. Less-Common Met. 126 (1986) 139.
[6] H.S. Kiliaan, Thesis, University Utrecht (1988).
[7] H.S. Kiliaan, A. Meijerink and G. Blasse, J. Lumin. 35 (1986) 155.
[8] A.J. de Vries, H.S. Kiliaan and G. Blasse, J. Sol. St. Chem. 65 (1986) 190.
[9] E. Gmelin, Handbuch der Anorganischen Chemie, Seltene Erdelemente, Teil C3 (1976) 295;
J.H. Burns, Inorg. Chem. 4 (1965) 881.
[10] A.J. de Vries, J.P.M. van Vliet and G. Blasse, Phys. Stat. Sol. (b) 149 (1988) 391.
[11] See e.g. R. Reisfeld and C.K. Jørgensen, in: Lasers and excited States of Rare Earths (Springer, Berlin, 1977) Ch. 2.
[12] S.A. Miller, H.E. Rast and H.H. Caspers, J. Chem. Phys. 52 (1970) 4172.
[13] J.M.F. van Dijk and M.F.H. Schuurmans, J. Chem. Phys. 78 (1983) 5317.
[14] A.J. de Vries and G. Blasse, J. Chem. Phys. 88 (1988) 7312.
[15] C.T. Garapon, B. Jacquier, J.P. Chaminade and C. Fouassier, J. Lumin. 34 (1986) 211.
[16] A.J. de Vries and G. Blasse, J. de Phys. 46 (C7) (1985) 109.
[17] L.R. Elias, W.S. Heaps and W.M. Yen, Phys. Rev. B8 (1973) 4989.
[18] A.J. de Vries, B.P. Minks and G. Blasse, J. Lumin. 39 (1988) 153.
[19] I.A. Bondar, A.I. Burshtein, A.V. Krutikov, L.P. Mezentseva, V.V. Osiko, V.P. Sakun, V.A. Smirnov and I.A. Shcherbakov, Sov. Phys. JETP 54 (1982) 45.
[20] A.I. Burshtein, Sov. Phys. Usp. 27 (1984) 579.
[21] J.T. Waber and D.T. Cromer, J. Chem. Phys. 42 (1965) 4116.
[22] W.T. Carnall, in: Handbook on the Physics and Chemistry of the Rare Earths, eds. K.A. Gschneidner Jr. and L. Eyring (North-Holland, Amsterdam, 1979) ch. 24.
[23] G.H. Dieke, in: Spectra and Energy Levels of Rare Earth Ions in Crystals (Wiley, New York, 1968).